# Optimal Charging of Electric Vehicles in Smart Grid: Characterization and Valley-Filling Algorithms

Niangjun Chen*, Tony Q.S. Quek†‡ and Chee Wei Tan§
*Department of Computer Science, California Institute of Technology, Pasadena, CA 91125 USA
†Institute for Infocomm Research, 1 Fusionopolis Way #21-01 Connexis, Singapore 138632
‡Singapore University of Technology and Design, Singapore
§Department of Computer Science, City University of Hong Kong, Hong Kong

***Abstract*—Electric vehicles (EVs) offer an attractive long-term solution to reduce the dependence on fossil fuel and greenhouse gas emission. However, a fleet of EVs with different EV battery charging rate constraints, that is distributed across a smart power grid network requires a coordinated charging schedule to minimize the power generation and EV charging costs. In this paper, we study a joint optimal power flow (OPF) and EV charging problem that augments the OPF problem with charging EVs over time. While the OPF problem is generally nonconvex and nonsmooth, it is shown recently that the OPF problem can be solved optimally for most practical power grid networks using its convex dual problem. Building on this strong duality result, we study a nested optimization approach to decompose the joint OPF and EV charging problem. We characterize the optimal offline EV charging schedule to be a valley-filling profile, which allows us to develop an optimal offline algorithm with computational complexity that is significantly lower than centralized interior point solvers. Furthermore, we propose a decentralized online algorithm that dynamically tracks the valley-filling profile. Our algorithms are evaluated on the IEEE 14 bus system, and the simulations show that the online algorithm performs almost near optimality ($<1\%$ relative difference from the offline optimal solution) under different settings.**

## I. Introduction

Electric vehicles (EVs) are getting more popular as a long-term vehicular technology to reduce the dependence on fossil fuel and the emission of greenhouse gases. However, with an increase in EV penetration, uncoordinated charging can lead to additional power losses and unacceptable voltage variation that overload the power grid. One way to tackle this problem is to adopt a "smart grid" solution, which allows EVs to communicate with the utility that coordinates their charging activities. Besides preventing grid overload, it has been shown that a coordinated EV charging can improve frequency regulation [1], smooth out the generation intermittency from renewable sources, and increase the efficiency in electricity usage [2], [3]. In this setting, we consider two types of load connected to the power grid network:

- *Price-inelastic load:* The exact power requested by this type of load must be provided. This corresponds to standard loads in a conventional grid such as lighting and heating.
- *Price-elastic load:* The power delivered to this type of load can vary depending on the current cost and a deadline. An example is the charging and recharging of EV batteries in a smart grid.

Considering these two types of loads, the two key problems that we study are: What is the optimal charging schedule for EVs to minimize the total power generation cost and EV charging cost? How to find a near optimal online algorithm if the future *price-inelastic load* is uncertain (due to the realistic causality constraint)? To formulate these problems, we leverage the well-known optimal power flow (OPF) problem and consider its time-dependent extension.

The solution of the OPF problem optimizes the operation of a power grid, and in general is NP-hard and nonconvex. However, the authors of [4] and [5] recently show that most practical power grid configurations surprisingly exhibit a useful property that guarantees zero duality gap between the OPF problem and its convex dual relaxation, thus making efficient polynomial time algorithm for the OPF problem possible.

To incorporate the time-varying electricity demand and *price elastic load*, we extend the OPF problem to a time-dependent OPF charging problem that spans over a scheduling period. It consists of a finite number of OPF subproblems coupled with one another by the constraint associated with the *price-elastic load*, e.g. the EV charging constraints. If a power grid configuration has zero duality gap for the OPF problem, then it has implications on how its time-dependent extension can be solved.

In this paper, we leverage the zero duality gap result in [4] to develop both offline and online algorithms that solve the joint OPF-EV charging optimization problem. To this end, we propose a nested optimization method that decomposes the joint OPF-EV charging problem into separable subproblems, and then solve the decoupled problem using a *nonsmooth separable programming* approach. The main contribution of the paper are as follows:

1) For time invariant EV charging cost, we characterize the offline optimal solution to be *valley-filling*. The valley-filling characterization holds true for all network configurations that guarantee the zero duality gap condition in the OPF problem.
2) We propose an offline algorithm that can solve the joint OPF-EV charging problem with a computational complexity lower than centralized interior point solvers.
3) To account for the causality constraint from the price-inelastic load, we propose an online algorithm that dynamically tracks this *valley-filling* characteristic. The online algorithm can be easily implemented in a decen-

TABLE I: Notations

| | |
|---|---|
| $\mathcal{N}$ | set of buses in the power grid network |
| $\mathcal{L}$ | set of transmission lines in the network |
| $\mathbf{Y}$ | admittance matrix |
| $f_k(\cdot)$ | convex cost function for bus $k$ |
| $\mathbf{p}[t]+\mathbf{q}[t]\mathbf{j}$ | complex vector of power generated at time $t$ |
| $\tilde{\mathbf{p}}[t]+\tilde{\mathbf{q}}[t]\mathbf{j}$ | complex vector of price-inelastic demand at time $t$ |
| $\hat{\mathbf{p}}[t]$ | nonnegative vector of EV charging rate at time $t$ |
| $\boldsymbol{\alpha}$ | nodal EV charging cost |
| $\mathbf{v}[t]$ | complex voltage vector at time $t$ |
| $\mathbf{W}[t]$ | $\mathbf{v}[t]\mathbf{v}[t]^*$ |
| $\bar{\mathbf{r}}[t], \underline{\mathbf{r}}[t]$ | charging rate limits at time $t$ |
| $\mathbf{c}$ | vector of total EV energy demand |
| $e_k$ | $k^{th}$ standard basis of $\mathbf{R}^{\lvert\mathcal{N}\rvert}$ |

tralized manner: at each time interval, charging decision is made locally by each vehicle after comparing its battery's charging rate limit to an estimated valley level set by the utility. We evaluate the performance of our algorithms under different settings of demand and EV penetration, and demonstrate that the performance of the online algorithm is near optimal.

The paper is organized as follows. Section II introduces the system model and problem formulation. Section III gives the main analytical results and valley-filling algorithms. Section IV gives the simulation results and the conclusion is given in Section V. We use $(\mathbf{x}[t])_j$ to represent the value of the $j^{th}$ component of a vector $\mathbf{x}[t]$ at iteration $t$. Due to space constraint, the key results in Section III are stated without proofs, and the detailed proofs can be found in [6].

## II. System Model and Problem Formulation

We consider a discrete-time model where the time-slot interval matches the timescale at which the power grid adjusts its power generation. Without loss of generality, the goal is to optimize the operation of the power grid over a time-interval of interest $t \in \{0, 1, \ldots, T\}$. Thus $T$ is the scheduling period duration. In practice, $T$ could be a day and a slot $t$ could be in the order of minutes. In addition, we assume that the loads are fixed over each time interval $[t, t+1]$.

### A. EV battery model

Suppose that each bus $k \in \mathcal{N}$ can connect to a price-inelastic load and a price-elastic EV battery. Furthermore, we assume that each EV battery can absorb or inject only active power at an adjustable rate via a smart outlet. In the following, we consider that each bus is connected to only one EV battery. However, our results can be generalized to the case when multiple EV batteries are co-located at the same bus.

Each smart outlet has a charging rate limit at each time $t$ [7], hence for $k \in \mathcal{N}$ and $t \in \{1, 2, \ldots, T-1\}$,

$$(\underline{\mathbf{r}}[t])_k \le (\hat{\mathbf{p}}[t])_k \le (\bar{\mathbf{r}}[t])_k, \tag{1}$$

and set $(\underline{\mathbf{r}}[t])_k = (\bar{\mathbf{r}}[t])_k = 0$ if no EV is connected to bus $k$ at time $t$. Let $B_k, s_k(0)$, and $\eta_k$ denote the battery capacity, initial state of charge (SOC), and charging efficiency, respectively. By the deadline $T$, the EV should be fully charged, hence, $\eta_k \sum_{t=1}^{T-1} (\hat{\mathbf{p}}[t])_k \Delta t = B_k(1 - s_k(0))$. Let $C_k := B_k(1-s_k(0))/(\eta_k \Delta t)$, then the EV charging constraint is the following, for all $k \in \mathcal{N}$

$$\sum_{t=1}^{T-1} (\hat{\mathbf{p}}[t])_k = \mathbf{c}_k. \tag{2}$$

### B. The joint OPF-EV charging problem

Using the EV battery model, we study the following time-dependent joint OPF-EV optimization problem:

$$\begin{aligned}
\min_{\{\mathbf{W}[t],\hat{\mathbf{p}}[t]\}} \; & \sum_{t=1}^{T-1}\sum_{k\in\mathcal{N}} f_k((\mathbf{p}[t])_k) + \sum_{t=1}^{T-1}\sum_{k\in\mathcal{N}} \boldsymbol{\alpha}_k (\hat{\mathbf{p}}[t])_k && \text{(3a)}\\
\text{s.t.} \; & P_k^{\min} \le (\mathbf{p}[t])_k \le P_k^{\max}, && \text{(3b)}\\
& Q_k^{\min} \le (\mathbf{q}[t])_k \le Q_k^{\max}, && \text{(3c)}\\
& (V_k^{\min})^2 \le \mathbf{W}[t]_{kk} \le (V_k^{\max})^2, && \text{(3d)}\\
& (\mathbf{W}[t]_{ll} - \mathbf{W}[t]_{lm})\mathbf{Y}_{lm}^* \le S_{lm}^{\max}, && \text{(3e)}\\
& \text{Trace}\{\mathbf{W}[t]\mathbf{Y}^* e_k e_k^*\} = (\mathbf{p}[t])_k - ((\hat{\mathbf{p}}[t])_k + (\tilde{\mathbf{p}}[t])_k) \\
& \qquad + ((\mathbf{q}[t])_k - (\tilde{\mathbf{q}}[t])_k)\mathrm{j}, && \text{(3f)}\\
& \mathbf{W}[t] \succeq 0, && \text{(3g)}\\
& \text{rank}(\mathbf{W}[t]) = 1, && \text{(3h)}\\
& \sum_{t=1}^{T-1} \hat{\mathbf{p}}[t] = \mathbf{c}, && \text{(3i)}\\
& \underline{\mathbf{r}}[t] \le \hat{\mathbf{p}}[t] \le \bar{\mathbf{r}}[t]. && \text{(3j)}
\end{aligned}$$

In the above, the physical limits $P_k^{\min}, P_k^{\max}, Q_k^{\min}, Q_k^{\max}, V_k^{\min}, V_k^{\max}$ and $S_{lm}^{\max}$ are given. Note that $f_k(\cdot)$ is the power generation cost function at bus $k$, and (3b)–(3h) are standard OPF constraints on power balance, voltage, and thermal limit of transmission lines. In addition, (3i) and (3j) are the EV charging constraints. We can set $P_k^{\min} = P_k^{\max} = Q_k^{\max} = Q_k^{\min} = 0$ if there is no generator at bus $k$. In (3a), we assume that the EV charging cost $\boldsymbol{\alpha}_k$ is time invariant.

### C. Decoupling power dispatching from EV scheduling

While the optimization variables in the joint OPF-EV charging problem (3) are $\mathbf{W}[t]$ and $\hat{\mathbf{p}}[t]$, if the optimal charging decision, $\hat{\mathbf{p}}[t]$ is also known, then all the remaining variables $\mathbf{W}[t]$ become separable in $t$. Hence, solving the joint OPF-EV charging problem at time $t$ is the same as solving the OPF problem with the demand given by$(\tilde{\mathbf{p}}[t] + \hat{\mathbf{p}}[t])$:

$$\begin{aligned}
F(\hat{\mathbf{p}}[t] + \tilde{\mathbf{p}}[t]) := \min_{\mathbf{W}[t]} & \left( \sum_{k\in\mathcal{N}} f_k((\mathbf{p}[t])_k) \right) \\
& \text{s.t. } (3\text{b}), (3\text{c}), \ldots, (3\text{h}).
\end{aligned} \tag{4}$$

Since the convex dual problem of the OPF can be efficiently solved [4], we can decouple the power dispatching, i.e., finding

$\mathbf{W}[t]$, from the EV scheduling, i.e., finding $\hat{\mathbf{p}}[t]$, and focus on the following EV scheduling problem:

$$\min_{\hat{\mathbf{p}}[t]} \quad \sum_{t=1}^{T-1} F\left(\hat{\mathbf{p}}[t] + \tilde{\mathbf{p}}[t]\right) + \boldsymbol{\alpha}^{\mathsf{T}} \hat{\mathbf{p}}[t] \tag{5a}$$

$$\text{s.t.} \quad \underline{\mathbf{r}}[t] \leq \hat{\mathbf{p}}[t] \leq \bar{\mathbf{r}}[t] \quad \forall t \in [1, T-1], \tag{5b}$$

$$\sum_{t=1}^{T-1} \hat{\mathbf{p}}[t] = \mathbf{c}, \tag{5c}$$

where $F(\hat{\mathbf{p}}[t] + \tilde{\mathbf{p}}[t])$ returns the optimal value of the OPF problem for a total load demand $(\tilde{\mathbf{p}}[t] + \hat{\mathbf{p}}[t])$.

## III. Valley-filling Algorithms

### A. Optimal Offline Algorithm for EV Scheduling Problem

The following result is a direct consequence of the zero duality gap property of the OPF problem, which reveals the convexity of the decoupled function in (4).

**Theorem 1.** *If the zero duality gap condition holds in* (4)*, then $F : \mathbb{R}^{|\mathcal{N}|} \to \mathbb{R}$, is a convex function.*

By convexity of $F$, and suppose that the charging rate constraints are inactive, we can apply Jensen's inequality and get the following result:

**Lemma 1.** *If $\forall t, \underline{\mathbf{r}}[t] = -\infty, \bar{\mathbf{r}}[t] = \infty$, then the EV scheduling problem* (5) *has an optimal solution $\hat{\mathbf{p}}[1] + \tilde{\mathbf{p}}[1] = \hat{\mathbf{p}}[2] + \tilde{\mathbf{p}}[2] = \ldots \hat{\mathbf{p}}[T-1] + \hat{\mathbf{p}}[T-1] = \mathbf{p_E} + \mathbf{p_I}$, where $\mathbf{p_E} = \left(\sum_{t=1}^{T-1} \hat{\mathbf{p}}[t]\right)/(T-1)$ and $\mathbf{p_I} = \left(\sum_{t=1}^{T-1} \tilde{\mathbf{p}}[t]\right)/(T-1)$.*

When the charging rate limits are inactive, the optimal solution is a *flat* profile, i.e., $\forall t, \hat{\mathbf{p}}[t] + \tilde{\mathbf{p}}[t]$ is constant. Next, we consider the case where the charging rate constraints can be active. The optimal solution will then no longer be *flat*, but *valley-filling* as defined in the following:

**Definition 1.** *A charging profile is valley-filling, if there exists a unique vector $\mathbf{a}$ such that $\hat{\mathbf{p}}[t] = [\mathbf{a} - \tilde{\mathbf{p}}[t]]_{\underline{\mathbf{r}}[t]}^{\bar{\mathbf{r}}[t]}, \forall t$, where $[x]_l^u = \max(l, \min(x, u))$.*

In the definition, $\mathbf{a}$ can be seen as a valley level that $\hat{\mathbf{p}}[t] + \tilde{\mathbf{p}}[t]$ tries to reach unless $\hat{\mathbf{p}}[t]$ is constrained by its charging rate limits. A similar definition of *valley-filling* for EV scheduling can be found in [8]. Interestingly, the *valley-filling* characterization is reminiscent of the *water-filling* notion for power allocation to maximize capacity in information theory [9].

The following theorem can be proved by using a substitution argument, i.e., if there is an optimal charging profile that is not *valley-filling*, then by convexity of $F$, we can always construct a *valley-filling* profile with the same or lower objective value.

**Theorem 2.** *For a general convex function $F(\cdot)$, a valley-filling profile is optimal to the EV Scheduling problem* (5)*.*

**Corollary 1.** *A valley-filling profile is a minimizer for any convex function $F(\cdot)$. For example, let $F(\hat{\mathbf{p}}[t] + \tilde{\mathbf{p}}[t]) = \left(\sum_{k \in \mathcal{N}} ((\hat{\mathbf{p}}[t])_k + (\tilde{\mathbf{p}}[t])_k)\right)^2$, we can see that the valley-filling profile is also minimizing the $l_2$ norm of the aggregate load. Furthermore, as the total load over time $\sum_{t=1}^{T-1} \sum_{k \in \mathcal{N}} (\hat{\mathbf{p}}[t])_k + (\tilde{\mathbf{p}}[t])_k$ is a constant, a valley filling profile is also a load variance minimizing profile.*

Next, we show the uniqueness of the valley level $\mathbf{a}$. Note that $\mathbf{a}$ must satisfy the following for $j = 1, \ldots, |\mathcal{N}|$:

$$\min_t \{(\tilde{\mathbf{p}}[t])_j + (\underline{\mathbf{r}}[t])_j\} \leq \mathbf{a}_j \leq \max_t \{(\tilde{\mathbf{p}}[t])_j + (\bar{\mathbf{r}}[t])_j\}, \tag{6a}$$

$$\sum_{t=1}^{T-1} \hat{\mathbf{p}}[t] = \sum_{t=1}^{T-1} [\mathbf{a} - \tilde{\mathbf{p}}[t]]_{\underline{\mathbf{r}}[t]}^{\bar{\mathbf{r}}[t]} = \mathbf{c}. \tag{6b}$$

If we look at (6b) component-wise, it is a continuous and strictly increasing function of $\mathbf{a}_j$ for $\mathbf{a}_j$ in the box constraint (6a). Since (6b) is continuous and strictly increasing, we can find a unique $\mathbf{a}$ via the bisection method for the offline case. This is presented in the following algorithm with $\varepsilon$ as an error tolerance level. We determine $\mathbf{a}$ in a component-wise manner. Each iteration of the `while` loop in the bisection algorithm will halve the search space for $\mathbf{a}_j$, and therefore the computational complexity of the bisection algorithm is low.

**Algorithm 1** Valley Level Bisection

$\forall j, \mathbf{u}_j \leftarrow \max_t\{(\tilde{\mathbf{p}}[t])_j + (\bar{\mathbf{r}}[t])_j\}$;
  $\mathbf{l}_j \leftarrow \min_t\{(\tilde{\mathbf{p}}[t])_j + (\underline{\mathbf{r}}[t])_j\}$;
**for** $j = 1 \to |\mathcal{N}|$ **do**
  **while** $(\|\mathbf{u}_j - \mathbf{l}_j\| \geq \varepsilon)$ **do**
    $\mathbf{m}_j \leftarrow \frac{1}{2}(\mathbf{u}_j + \mathbf{l}_j)$;
    **if** $(\sum_{t=1}^{T-1} [\mathbf{m}_j - (\tilde{\mathbf{p}}[t])_j]_{(\underline{\mathbf{r}}[t])_j}^{(\bar{\mathbf{r}}[t])_j} > \mathbf{c}_j)$ **then**
      $\mathbf{u}_j \leftarrow \mathbf{m}_j$;
    **else**
      $\mathbf{l}_j \leftarrow \mathbf{m}_j$;
$\mathbf{a} \leftarrow \mathbf{m}$.

**Remark 1.** *Once $\mathbf{a}$ is determined, solving $\hat{\mathbf{p}}[t]$ can be done in $O(1)$ time. Thus, the joint OPF-EV charging problem* (3) *reduces from a semidefinite program (SDP) with $O((|\mathcal{N}| + |\mathcal{L}|)(T-1))$ variables to $(T-1)$ SDPs each with $O(|\mathcal{N}| + |\mathcal{L}|)$ variables. Since the complexity of SDP interior point algorithms grows superlinearly with respect to the number of variables [10], [11], this decomposition leads to a lower computational complexity.*

The offline algorithm for the EV Scheduling problem (5) is shown in the following.

**Algorithm 2** Offline EV Scheduling

Calculate the valley level $\mathbf{a}$ using Algorithm 1;
**for** $t = 1 \to T-1$ **do**
  $\hat{\mathbf{p}}[t] \leftarrow [\mathbf{a} - \tilde{\mathbf{p}}[t]]_{\underline{\mathbf{r}}[t]}^{\bar{\mathbf{r}}[t]}$;
  Solve the OPF problem with the active load demand set to $(\hat{\mathbf{p}}[t] + \tilde{\mathbf{p}}[t])$;

### B. Online Algorithm for EV Scheduling Problem

Under a causality constraint, we do not assume any knowledge of $\tilde{\mathbf{p}}[t]$ until time $t$. Therefore, we cannot use the previous bisection algorithm to find $\mathbf{a}$ in an online fashion. Instead, we propose an algorithm that estimates the valley level, which is denoted by $\mathbf{a}'[t]$ and adjusts it dynamically in an online fashion. This is illustrated in Algorithm 3.

**Algorithm 3** Online EV Scheduling

1: $\mathbf{a}'[1] \leftarrow \mathbf{p_E} + \widehat{\mathbf{p_I}}$; $\quad$ ($\widehat{\mathbf{p_I}}$ is an estimation of $\mathbf{p_I}$)
2: **for** $t = 1 \to T-1$ **do**
3: $\quad \hat{\mathbf{p}}[t] \leftarrow [\mathbf{a}'[t] - \tilde{\mathbf{p}}[t]]_{\underline{\mathbf{r}}[t]}^{\bar{\mathbf{r}}[t]}$;
4: $\quad$ **for** $j = 1 \to |\mathcal{N}|$ **do**
5: $\quad\quad$ **if** $(\sum_{k=1}^{t}(\hat{\mathbf{p}}[k])_j > \mathbf{c}_j - \sum_{l=t+1}^{T-1}(\underline{\mathbf{r}}[l])_j)$ **then**
6: $\quad\quad\quad (\hat{\mathbf{p}}[t])_j \leftarrow \mathbf{c}_j - \sum_{l=t+1}^{T-1}(\underline{\mathbf{r}}[l])_j - \sum_{k=1}^{t-1}(\hat{\mathbf{p}}[k])_j$;
7: $\quad\quad$ **if** $(\sum_{k=1}^{t}(\hat{\mathbf{p}}[k])_j < \mathbf{c}_j - \sum_{l=t+1}^{T-1}(\bar{\mathbf{r}}[l])_j)$ **then**
8: $\quad\quad\quad (\hat{\mathbf{p}}[t])_j \leftarrow \mathbf{c}_j - \sum_{l=t+1}^{T-1}(\bar{\mathbf{r}}[l])_j - \sum_{k=1}^{t-1}(\hat{\mathbf{p}}[k])_j$;
9: $\quad\quad$ **if** $(t < T-1)$ **then**
10: $\quad\quad\quad (\mathbf{a}'[t+1])_j \leftarrow (\mathbf{a}'[t])_j + \frac{(\mathbf{a}'[t])_j - (\hat{\mathbf{p}}[t])_j - (\tilde{\mathbf{p}}[t])_j}{T-1-t}$;
11: $\quad$ Solve the OPF problem with the active load demand set to $(\hat{\mathbf{p}}[t] + \tilde{\mathbf{p}}[t])$;

For Algorithm 3, line 1 initializes the first estimation of $\mathbf{a}$. From Lemma 1, the ideal valley level is indeed $(\mathbf{p_E} + \mathbf{p_I})$ if the charging rate constraints are not active. We know the value of $\mathbf{p_E}$, which is just the charging target $\mathbf{c}$ divided by time $(T-1)$, but the value of $\mathbf{p_I}$ has to be estimated, possibly by learning from historical record of the price-inelastic load. Line 3 follows the valley-filling characterization outlined in the previous section. However, as the valley level estimation is not perfect, we need to take extra steps from line 5 to line 8 to ensure the feasibility of the solution. The rationale for line 5 to 6 is to ensure that the charging profile $(\hat{\mathbf{p}}[1], \ldots, \hat{\mathbf{p}}[T-1])$ will not overcharge the EV batteries at any point in time. Roughly speaking, it means that "if from this instance on, even charging at the minimal rate will eventually overcharge the EV batteries, then slow down the current charging rate." Line 7 to 8 are based on similar rationale and this prevents undercharging. Lastly, the estimation of the valley level is updated from line 9 to 10.

**Remark 2.** *Algorithm 3 can be efficiently implemented in a decentralized manner: at the beginning of iteration $t$, the utility broadcasts the estimated valley level $\mathbf{a}'[t]$, and each EV runs line 3 to line 8 and replies with its charging power. The utility collects $\hat{\mathbf{p}}[t]$ and runs line 9 to line 10 to calculate the next estimated valley level $\mathbf{a}'[t+1]$.*

The following result demonstrates the feasibility of the output from Algorithm 3.

**Theorem 3.** *If the charging rate constraints $(\bar{\mathbf{r}}[1], \ldots, \bar{\mathbf{r}}[T-1])$ and $(\underline{\mathbf{r}}[1], \ldots, \underline{\mathbf{r}}[T-1])$ permit a feasible solution, then $(\hat{\mathbf{p}}[1], \ldots, \hat{\mathbf{p}}[T-1])$ obtained from Algorithm 3 is a feasible solution to* (5).

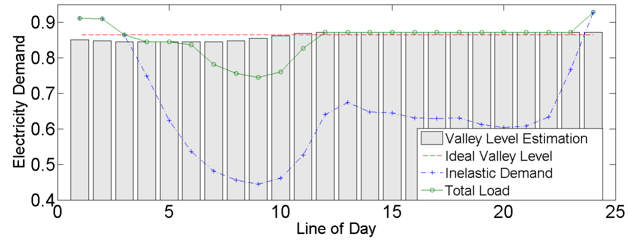


(a) Illustration of dynamic estimation of valley level

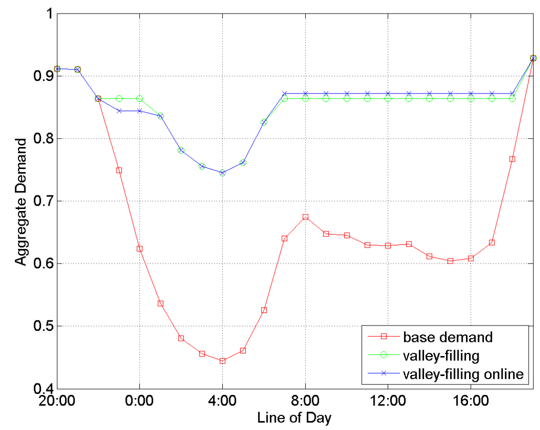


(b) Comparison of online and offline solution

Fig. 1: The base demand curve is the average residential load in the service area of SCE from 20:00 on Feb. 13th to 19:00 on Feb 14th, 2011 [12]. The valley-filling curve is obtained using Algorithm 2. The valley-filling online curve is obtained using Algorithm 3.

**Remark 3.** *Once the condition in line 5 is triggered, the subsequent charging rate will stay at the minimum. Similarly, once the condition in line 7 is triggered, the subsequent charging rate will stay at the maximum.*

While line 5 to line 8 ensure feasibility, we may not want to trigger those "if" conditions, because once any of them holds true, it means that there is no room left for optimization. Line 9 to line 10 achieve this by updating $\mathbf{a}'[t]$ based on the information up to iteration $t$. If the sum of the EV load and the price-inelastic load cannot meet the current valley level estimation $\mathbf{a}[t]$, then the next estimation $\mathbf{a}[t+1]$ will be adjusted in the opposite direction to ensure that $\sum_{t=1}^{T-1} \hat{\mathbf{p}}[t] = \mathbf{c}$.

As shown in Fig. 1a, the valley level estimation decreases when the sum of the EV load and the price-inelastic load exceeds the current estimation; it increases when the sum is below the estimation, and it stays the same when the sum meets the estimated level. This behavior is dictated by line 10, which updates the estimation in order to spread out the current error to subsequent estimated valley levels. The result below shows that with this dynamic adjustment, the "if" conditions in line 5 and line 7 will be inactive in most cases when the first estimation of the valley level is sufficiently good.

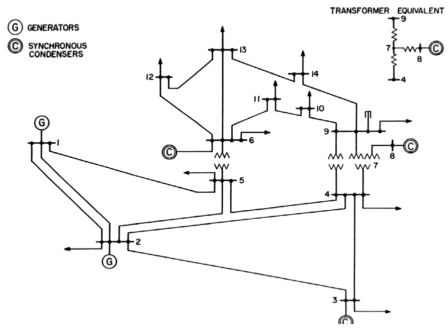


Fig. 2: IEEE 14-bus system studied in Section IV and taken from the IEEE power system test archive [14].

**Theorem 4.** *Assuming the estimation of* $\mathbf{p_I}$ *is correct, and* $\hat{\mathbf{p}}[T-1] = \mathbf{a}'[T-1] - \tilde{\mathbf{p}}[T-1]$*, then the charging profile* $(\hat{\mathbf{p}}[1], \ldots, \hat{\mathbf{p}}[T-1])$ *obtained from Algorithm 3 without line 5 to 8 is a feasible solution to the EV scheduling problem* (5).

Fig. 1b compares the EV charging profiles produced by Algorithm 2 and Algorithm 3. As illustrated, both exhibit the valley-filling characteristic, but the valley level of Algorithm 3 is changing dynamically.

## IV. Numerical Results

Consider the IEEE 14-bus system depicted in Fig. 2, where the circuit specifications and the physical limits are given in the library of the toolbox MATPOWER [13]. The system has five generators connected to buses 1, 2, 3, 6, and 8. Assume that each of the non-generator bus 4, 5, 7, 9, 10, 11, 12, 13, and 14 is connected to an EV load. Enumerate the batteries of these vehicles as $1, 2, \ldots, 9$. Consider that all the batteries are plugged in at time $t = 1$ and must be fully charged by time $T = 25$, the charging rate of each battery can be controlled only at the discrete time instants $1, 2, \ldots, 24$.

Aside from the elastic EV loads, suppose that each bus $k \in \{1, 2, \ldots, 14\}$ is connected to a price-inelastic load as well, which varies at the discrete times $1, 2, \ldots, 24$ according to

$$(\tilde{\mathbf{p}}[t])_k = \frac{l(t) \times P_k}{\overline{l(t)}}, \quad t = 1, 2, \ldots, 24, \tag{7}$$

where $(P_1, \ldots, P_{14})$ is equal to the load profile given in the library of the toolbox MATPOWER for the IEEE 14-bus system, $l(t)$ follows the average residential load in the service area of SCE at different times of the day (cf. SCE website [12]), and $\overline{l(t)} = \sum_{t=1}^{24} l(t)$. The goal is to optimize the controllable parameters of the power grid network such as the active power supplied by a generator or the charging rate of a battery, which can be modified only at the time instants $1, 2, \ldots, 24$. To this end, we aim to minimize the following cost function:

$$\sum_{t=1}^{24} \sum_{k \in \mathcal{N}} (\mathbf{p}[t])_k + \sum_{t=1}^{24} \sum_{k \in \mathcal{N}} \alpha(\hat{\mathbf{p}}[t])_k. \tag{8}$$

This cost function has the following features:

- The generation cost is the total active power generated by all the generators over the time horizon [1,24].
- The pricing vector of each battery is assumed to be independent of its bus number and invariant over time, and we let $\alpha = 2$ in the following.

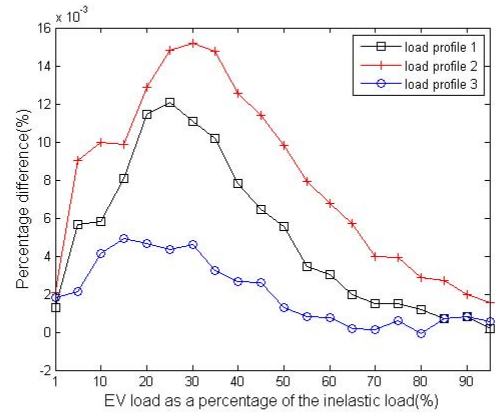


Fig. 3: Profile 1: residential load from 10:00 on Jul. 6th to 9:00 on Jul. 7th; Profile 2: average residential load from 15:00 on Aug. 27th to 14:00 on Aug. 28th; Profile 3: residential load from 1:00 on Mar. 11th to 0:00 on Mar. 12th. All load profiles are taken from SCE website [12].

### A. Effect of EV penetration

In this case, we vary the EV load to be from $10\%$ to $100\%$ of the price-inelastic load, and compute the percentage difference given by $(p^*_{\text{online}} - p^*_{\text{offline}})/p^*_{\text{offline}} \times 100$, where $p^*_{\text{offline}}$ is the optimal value of (8) obtained using Algorithm 2 and $p^*_{\text{online}}$ is the result from the Algorithm 3. Fig. 3 shows the simulation results using three different 24-hour load profiles taken randomly from the SCE residential load data [12]. Firstly, Algorithm 3 is able to produce charging profiles that almost optimally solve the joint OPF-EV charging problem (3). From the three randomly chosen load profile, the worst performance is less than $0.016\%$ different from the optimal value. Secondly, we can see all three plots go up initially and eventually decrease. This is because at the beginning, the EV load is relatively insignificant, and thus Algorithm 2 and 3 perform almost the same as there is little to optimize. As the EV load becomes more significant, the performance gap grows because Algorithm 3 lacks perfect knowledge. However, a higher EV penetration will also lead to larger room for optimization. Hence, the performance gap decreases and eventually approaches zero as the EV penetration increases.

### B. Effect of online estimation

In this example, the EV charging profile of a working example is illustrated. The price-inelastic load variation is based on the residential load profile from 15:00 on Aug. 27th to 14:00 on Aug. 28th (taken from the SCE website [12]). The EV penetration level is set to 50%, and we assume that there is 10% error in over estimating the initial valley level for

Algorithm 3, i.e., $\mathbf{a}'[1] = 1.1 \times \mathbf{a}$. Fig. 4a and Fig. 4b show the charging profile of one of the EVs produced by Algorithm 2 and Algorithm 3 respectively in this setting. We can make several observations from Fig. 4a and Fig. 4b:

1) An over-estimation of the initial valley level $\mathbf{a}'[1]$ causes Algorithm 3 to charge the EV batteries faster than optimum. As a result, the EV battery at bus 7 is fully charged two time slots before the deadline.
2) The result of the Algorithm 3 is still very close to the optimal value, as the percentage difference $(p^*_{\text{online}} - p^*_{\text{offline}})/p^*_{\text{offline}} \times 100\% = 0.0627\%$. Hence, in terms of power loss minimization, Algorithm 3 performs nearly optimally at this setting.

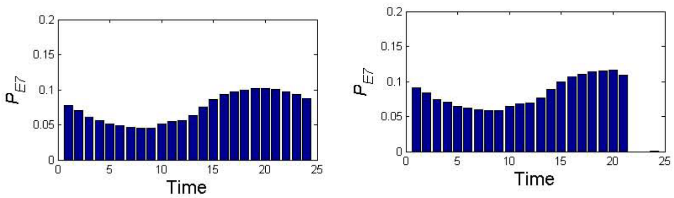


(a) Offline solution for EV at bus 7 (b) Online solution for EV at bus 7

Fig. 4: Comparison of EV charging profile for Algorithm 2 and Algorithm 3, $p^*_{\text{offline}} = 79.5348\text{pu}$, $p^*_{\text{online}} = 79.5847\text{pu}$.

### C. Runtime comparisons

In this section, we compare the computational time of the SDP optimization approach that uses interior point algorithm to solve (3) in [15] with that of Algorithms 2 and 3. The simulation is run on the IEEE 14 bus system for $T = 6, 12, 24, 48$ respectively.[1] The computational time measured is the average of running the respective algorithm for ten times.

TABLE II: Performance comparisons

| $T$ | SDP Optimization | Algorithm 2 | Algorithm 3 |
|---|---|---|---|
| 6 | 6.0 s | 5.8 s | 5.9 s |
| 12 | 13.1 s | 11.6 s | 11.6 s |
| 24 | 31.5 s | 22.9 s | 22.8 s |
| 48 | 84.0 s | 45.8 s | 45.7 s |
| 96 | 262.6 s | 87.5 s | 87.4 s |

From Table II, we see that the time complexity of Algorithm 2 and Algorithm 3 are comparable. Also, both Algorithm 2 and Algorithm 3 have lower time complexity as compared to the SDP optimization method in [15], and the saving in computational time from using Algorithm 2 and Algorithm 3 is more significant as $T$ increases. This demonstrates the advantage of the decoupling approach to solve the joint OPF-EV charging problem.

## V. Conclusion

We studied a time-dependent OPF charging problem that optimized jointly the operation of the power grid and the charging activity of electric vehicles. We proved that this problem is convex with respect to the total electricity demand, characterized the valley-filling charging profile to be optimal under constant electricity price, and proposed a decentralized online algorithm that followed this characterization. At each iteration of the online algorithm, each electric vehicle calculated its own charging rate according to the valley level broadcast by the utility, and the utility guided their charging rate by updating the valley level. Simulation results showed that the online algorithm performed almost optimally in minimizing power loss, and the optimal value of the online algorithm approached to that of the offline solution as the penetration of EVs increases.

In this paper, the online algorithm considers a time invariant pricing scheme. That is, the nodal electricity price remains constant throughout the scheduling period. However, when there are renewable sources, electricity prices can vary in real time. In addition, electric vehicles may require charging at different times in a more dynamical setting. Incorporating real time pricing, modeling vehicle arrivals as random events and accounting for the additional uncertainties with these extensions are interesting directions for future research.

## VI. Acknowledgement

The authors gratefully acknowledge helpful discussions with Steven H. Low at Caltech.

## References

[1] S. Han, S. Han, and K. Sezaki, "Development of an optimal vehicle-to-grid aggregator for frequency regulation," *IEEE Trans. on Smart Grid*, vol. 1, no. 1, pp. 65–72, June 2010.
[2] A. Boulanger, A. Chu, S. Maxx, and D. Waltz, "Vehicle electrification: Status and issues," *Proc. IEEE*, vol. 99, no. 6, pp. 1116–1138, June 2011.
[3] O. Sundstrom and C. Binding, "Flexible charging optimization for electric vehicles considering distribution grid constraints," *IEEE Trans. Smart Grid*, vol. 3, no. 1, pp. 26 –37, March 2012.
[4] J. Lavaei and S. Low, "Zero duality gap in optimal power flow problem," *IEEE Trans. Power Syst.*, vol. 27, no. 1, pp. 92–107, February 2012.
[5] S. Bose, D. F. Gayme, S. Low, and K. M. Chandy, "Optimal power flow over tree networks," in *Proc. IEEE Allerton Conf. on Communication, Control and Computing*, September 2011.
[6] N. Chen, C. W. Tan, and T. Q. S. Quek, "Optimal charging of electric vehicles in smart grid: Characterization and valley-filling algorithms," August 2012, arXiv:1208.4743.
[7] A. Ipakchi and F. Albuyeh, "Grid of the future," *IEEE Power Energy Mag.*, vol. 7, no. 2, pp. 52–62, March-April 2009.
[8] L. Gan, U. Topcu, and S. Low, "Optimal decentralized protocol for electric vehicle charging," *IEEE Trans. Power Syst.*, 2012, to appear.
[9] T. Cover and J. Thomas, *Elements of Information Theory*. Wiley-Interscience, 2006.
[10] L. Vandenberghe and S. Boyd, "Semidefinite programming," *SIAM Review*, vol. 38, pp. 49–95, 1996.
[11] L. Porkolab and L. Khachiyan, "On the complexity of semidefinite programs," *Journal of Global Optimization*, vol. 10, pp. 351–365, June 1997.
[12] "Southern California Edison website." [Online]. Available: http://www.sce.com/005_regul_info/eca/DOMSM11.DLP
[13] R. D. Zimmerman, C. E. Murillo-Sánchez, and R. J. Thomas, "MATPOWER: Steady-state operations, planning and analysis tools for power systems research and education," *IEEE Trans. Power Syst.*, vol. 26, no. 1, pp. 12–19, February 2011.
[14] R. Christie, "Power systems test case archive." [Online]. Available: http://www.ee.washington.edu/research/pstca
[15] S. Sojoudi and S. Low, "Optimal charging of plug-in hybrid electric vehicles in smart grids," in *Proc. IEEE Power and Energy Society General Meeting*, July 2011, pp. 1–6.

[1] We used MATLAB version 7.6.0.324 (R2008a). The programs were run on an Intel Xeon CPU 2.80GHz machine running on Windows 7 OS.